International Journal of Advanced Engineering Research and Science (IJAERS)
Peer-Reviewed Journal
ISSN: 2349-6495(P) | 2456-1908(O)
Vol-11, Issue-9; Sep, 2024
Journal Home Page Available: https://ijaers.com/
Article DOI: https://dx.doi.org/10.22161/ijaers.119.3

Research on heat transfer model prediction of Tesla Valve heat sink based on training neural network method

Yan-Xiao Jia, Yan-Zuo Chang*, Guo-Xing Yang, Ruo-Yu Yang, Yi-wei Zhang, Ting-Hao Zhang

Energy and Power Engineering, Guangdong University of Petrochem Technology (GDUPT), Maoming,525000,China
(Corresponding author: Yan-Zuo Chang PhD), Email: qq3102492448@163.com

Received: 12 Aug 2024,

Receive in revised form: 12 Sep 2024,

Accepted: 19 Sep 2024,

Available online: 23 Sep 2024

***Keywords*— Tesla valve heat sink, neural network, CFD numerical simulation.**

***Abstract*— With the increasing power density of electronic equipment, heat dissipation technology has become the key to ensure the stable operation of equipment. Because of its unique structural design, the Tesla valve heat sink shows great potential in the heat dissipation of high-power electronic devices. However, the traditional heat transfer model prediction method has the problems of complex calculation and low efficiency. The purpose of this study is to explore a method of heat transfer model prediction based on training neural network to improve the accuracy and efficiency of heat transfer efficiency prediction of Tesla valve heat sink. The heat transfer data of Tesla valve heat sink under different structures were collected by numerical simulation. The data were then used to train a feed forward neural network. Through a lot of training and verification, the neural network model shows good generalization ability and can accurately predict the heat transfer efficiency under unknown conditions. In this study, the effects of network structure, training algorithm and optimization strategy on model performance are discussed, and an improved network architecture is proposed to improve the accuracy of prediction. Finally, the advantages of the proposed method in computational efficiency and prediction accuracy are verified by comparison with traditional methods.*

I. INTRODUCTION

In the rapid development of electronic technology, the performance leap of high-power density electronic devices is closely related to the improvement of heat dissipation efficiency [1]. With the miniaturization and high frequency of integrated circuits and the continuous rise of computing speed, the heat generated inside electronic devices has increased sharply, and the heat dissipation problem has become one of the key factors restricting its performance bottleneck. With its unique geometric structure and excellent heat transfer performance, the Tesla valve heat sink is considered as one of the new generation of efficient heat dissipation solutions [2].

The Tesla valve, through a carefully designed asymmetric flow channel structure, enables the fluid to flow efficiently in a specific direction, while being significantly hindered in the opposite direction. This feature not only improves the heat dissipation efficiency, but also reduces energy consumption, providing a strong guarantee for the efficient and stable operation of electronic equipment. Domestic and foreign scholars continue to deepen the research of Tesla valve, from the basic flow characteristics analysis to the complex heat transfer performance optimization, each progress indicates its broad application prospects in the future heat dissipation technology.

At present, the research of Tesla valve has covered multiple dimensions. The study of Thompson et al. [3] revealed the effects of valve spacing, series and Reynolds number on the performance of multistage Tesla valves, providing a theoretical basis for design optimization [3]. S.F. de Vries et al. verified the feasibility of the new Tesla valve in enhancing heat transfer through innovative design, combined with steady-state two-phase flow experiment and laminar single-phase simulation, and further promoted the application of Tesla valve in high-efficiency heat dissipation systems such as heat pipes [4]. Based on the Fluent simulation platform, Ren Pu studied the fluid flow characteristics of the Tesla valve during reverse navigation, and also analyzed the causes of cavitation in the Tesla valve and the influence of the cavitation model on the fluid flow [9]. In recent years, artificial intelligence technology and neural network technology have provided new possibilities to solve this problem.

In the early 1990s, the personal computer (PC) era was represented by the Intel 80486 microprocessor (486 era), the CPU power consumption is relatively low, such as the maximum power consumption of Intel 486DX4 processor reached 5W, the heat dissipation demand is not high, the design of the radiator is usually more simple, generally using the passive heat dissipation of static heat sink, or equipped with a small fan to achieve active heat dissipation. With the increase of CPU frequency, such as the introduction of Intel Pentium series, power consumption and heat began to increase, and power consumption was also greatly increased to 11.2w, and the radiator began to be equipped with a fan, forming the prototype of an air-cooled radiator. In the Pentium III and IV era, the power consumption and heat output of the CPU increased sharply, and the volume of the radiator increased accordingly, and copper base, plug copper and copper-aluminum combined fin radiator appeared to improve the heat dissipation efficiency.

However, the complex structure of Tesla valve makes its flow and heat transfer mechanism difficult to be fully explained by traditional theories, especially under complex conditions such as high flow rate and multiphase flow, its performance prediction and optimization face many difficulties. In addition, existing prediction models often rely on large amounts of experimental data, which are expensive to compute and difficult to respond quickly to design changes.

To solve these problems, artificial intelligence technology and neural network technology are introduced in this study. Because of its powerful nonlinear mapping ability and self-learning ability, neural network can construct accurate prediction model. The prediction method of heat transfer mode of Tesla valve heat sink based on training neural network is the concrete practice of this idea. We aim to explore a method for predicting heat transfer mode of Tesla valve heat sink based on training neural network, in order to improve the accuracy and computational efficiency of prediction [5][6][7][8].

In this paper, CFD numerical simulation technology is first used to build a variety of Tesla valve models, and simulation analysis is carried out under the same working conditions, and detailed heat transfer data including inlet and outlet pressure difference, Nussel number, and geometric structure parameters are collected. These data will serve as the "nourishment" for neural network training and provide a solid foundation for model construction.

A feedforward neural network is then designed and trained, which realizes complex mapping of the heat transfer performance of the Tesla valve through the connection and activation of multiple layers of neurons. In the training process, the network structure is optimized and the hyperparameters are adjusted to improve the prediction accuracy and generalization ability of the model. At the same time, the influence of two key parameters, the length of the flow channel section and the Angle of the valve, on the heat transfer performance is studied, and a new way to optimize the structure of the Tesla valve is explored by adjusting these parameters.

This study is expected to establish a set of neural network-based heat transfer performance prediction model of Tesla valve heat sink, which can accurately and efficiently predict heat transfer performance of different structures of Tesla valves, and provide strong support for the design and optimization of heat sink.

As an important cooling element in electronic products, the development history of electronic heat sink closely follows the evolution of electronic technology. With the improvement of the performance of electronic products, heat dissipation technology is also constantly improving and innovating [10].

The research significance of this paper comes from the use of CFD numerical simulation to collect heat transfer data of different Tesla valve models under the same working conditions, including inlet and outlet pressure difference, Nussel number, geometric structure parameters, etc. Then design and train a feedforward neural network, establish a training model, and adjust the grid structure. The influence of two parameters, the length of the flow channel section and the Angle of the valve, on the heat transfer performance of the Tesla valve was studied, and the optimization algorithm was finally able to improve the generalization ability and prediction accuracy of the model. The prediction model was used to predict the heat transfer performance of different structures and optimize the structure of the Tesla valve [11][12].

II. TESLA VALVE MODEL ESTABLISHMENT AND CFD PRE-TREATMENT

Since Tesla valves are mostly used in electronic products, the size of the design in this paper will be determined according to the size of electronic products. CAD is used to establish a two-dimensional geometric model, and 3D is generated by the built-in modeling tool in ANSYS2022. Then Mesh in ANSYS2022 is used to divide the model and name the boundary.

2.1 Initial selection of the Tesla valve geometry model

The average length of the Tesla valve designed in this paper is 100mm. As shown in Figure 1, the width of the flow channel section is fixed at 3mm, the length is D, and the valve Angle is α. These two geometric parameters change within the specified range, while the remaining parameters remain unchanged. Each Tesla valve is a one-stage, and this paper designs a two-stage Tesla valve. The fluid in the channel is water, and its physical properties change with temperature. Wall material is copper.

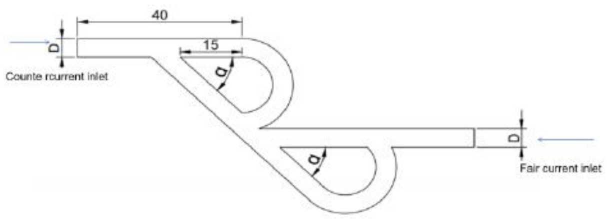

Fig. 1: Sample size of Tesla valve/mm

Tesla valve in the counter current process will appear some unique fluid mechanics phenomena, these phenomena are the result of its unique geometric structure and the physical characteristics of the fluid. Some key hydrodynamic phenomena such as increased flow rate, decreased pressure, cavitation effect, eddy current formation, fluid separation, enhanced heat exchange, flow asymmetry, turbulent transition, hydrodynamic instability, and energy dissipation may occur during the counter current process of the Tesla valve.

The speed of the upstream inlet and the upstream inlet is 0.05m/s, and the rest remain unchanged. The exit domain is set as the exit boundary. The fluid can effectively avoid the wing-like barrier and flow from the right to the left unimpeded, and the effect of acceleration is obtained due to the flow pressure, and the speed has been accelerating in the main channel, the speed is close to 0.1m/s; When fluid flows in reverse, it encounters a wing-like barrier. Whenever fluid passes through one of these channels, it flows into a wing-like barrier due to inertia. The shock of back flow and the sudden increase in pressure can prevent the fluid from moving forward, making it difficult to pass through the valve. The more wing-shaped obstacles, the more resistance the fluid is subjected to in the reverse flow, which creates the one-way flow characteristics of the Tesla valve.

A monitoring point is provided at the reverse flow inlet through road, near the oblique channel, to monitor the speed and pressure at the point.

III. NEURAL NETWORK

Artificial neural network (ANN) or analog neural network (SNN). These networks consist of interconnected neurons, divided into input layers, one or more hidden layers, and output layers, where neurons perform mathematical operations on input data and pass the results to the next layer, allowing the network to learn complex patterns and relationships in the data. Each node in the neural network receives input processing and passes the output to the next node[13] [14] [15].

Import Fluent simulation data results into the MATLAB workspace. The four data of upstream Nuf, counter-current Nur, relative performance evaluation standard RPEC and Di are imported into the work area as labels, and the output form is a numerical matrix, denoted as "T". The length of the section of the flow channel and the Angle of the valve are imported into the work area as features, and the output form is a numerical matrix, denoted as "X"; Set several sets of parameters as shown in Table 1, and import them into the work area as prediction objects. The output form is a numerical matrix, which is denoted as "YC".

Table.1: Predicted parameters

Forecasting group	The length of the flow channel section/mm	Valve Angle/°
Forecasting 1	3	33
Forecasting 2	5	44
Forecasting 3	7	55
Forecasting 4	7	33
Forecasting 5	5	55
Forecasting 6	3	44

There are 9 samples in total. The 9 samples are divided into three parts: 70% training set, 15% verification set and 15% test set. In other words, 7 samples are taken as training set, 1 sample as verification set and 1 sample as test set. Using the least square method, it occupies a large memory, takes the least time, and can be automatically stopped. The results include Neural Network part, Algorithms part, Progress part and Plot part.

Save the trained neural network model, use the training model to predict the previously designed prediction parameters, and get the result "Y". The results are summarized in Table 4.

IV. INTERPRETATION OF RESULT

4.1 Fluent Simulation result analysis

Table 2 Simulated result

Experim-ental group	Downstr-eam pressure drop Δ Pf /Pa	Counterc-urrent pressure drop Δ Pr/Pa	Downstr-eam Nuf	Counterc-urren Nur	Di	RPEC
Test1	20.56	22.37	197.06	203.06	1.088	1.002
Test2	21.69	23.19	172.45	178.54	1.069	1.013
Test3	24.46	25.47	140.26	143.3	1.041	1.008
Test4	14.59	15.76	208.09	216.62	1.08	1.015
Test5	16.11	17.5	185.05	194.68	1.086	1.024
Test6	18.33	19.6	152.37	159.93	1.069	1.026
Test7	12.87	14.09	237.92	247.3	1.095	1.008
Test8	14.34	15.76	215.13	226.38	1.099	1.02
Test9	16.42	17.57	179.63	188.93	1.07	1.028

Table 3 Forecast summary

Forecasting group	Fair current Nuf	Adverse current Nur	Di	RPEC
Forecasting 1	196.5961	202.6147	1.0858	1.0038
Forecasting 2	188.0456	198.3291	1.0925	1.0245
Forecasting 3	183.1189	191.6469	1.0669	1.0249
Forecasting 4	235.6566	246.1588	1.0942	1.0098
Forecasting 5	164.1569	170.9464	1.0734	1.0235
Forecasting 6	176.9233	183.1591	1.0717	1.0075

Upflow Nu and counter flow Nur vary as the valve Angle increases. When the valve Angle is small, the Nu value is higher and the heat transfer effect is better. This may be because the smaller valve Angle helps the fluid form more vortex and turbulence inside the Tesla valve, which enhances heat transfer. However, as the valve Angle increases, the Nu value decreases, which may be due to the energy loss caused by the increase in the fluid flow path. The pressure drop data show that the down-flow pressure drop ΔPf and the counter-flow pressure drop ΔPr decrease as the valve Angle increases. This may be because the larger valve Angle helps the fluid flow through the valve more smoothly, reducing the resistance of the fluid. However, too low a valve Angle can result in too large a pressure drop, which can affect the overall performance of the Tesla valve. RPEC is used as a comparison of the overall performance of the Tesla valve in reverse flow and forward flow, and the closer the value is to 1, the better the performance. The RPEC value does not monotonically increase with increasing cross section length, which indicates that the design of the Tesla valve needs to find a balance between heat transfer efficiency and fluid flow resistance. The Di parameter is used as a measure of single flow, and its value reflects the resistance of the valve to counter current. As shown in Table 3, Di values are lower in some test groups, which may mean that these Tesla valve designs are more effective at preventing backflow.

The length of the cross section also affects the performance of the Tesla valve. Increasing the cross section length helps to increase the Nu value and thus the heat transfer performance, but it may also lead to an increase in pressure drop. This shows that when designing the Tesla valve, it is necessary to consider the heat transfer efficiency and the resistance of the fluid flow to achieve the optimal design. In summary, the valve Angle of the Tesla valve and the cross section length of the flow channel have a significant impact on its heat transfer performance. Smaller valve Angle is beneficial to increase Nu value, but may lead to increased pressure drop. The larger cross section length helps to improve the heat transfer performance, but may be unfavorable to the single conduction. Therefore, the design of the Tesla valve needs to consider multiple factors, by optimizing the valve Angle and cross section length to balance the heat transfer efficiency and fluid flow resistance to achieve the best heat dissipation results. In addition, the difference between the predicted results of the neural network model and the simulated data suggests that the model may require more training data or a more complex network structure to improve the prediction accuracy. Future research could further explore the optimal combination of these parameters and optimize the design of the Tesla valve through experimental validation.

The parts of Tesla valve where heat transfer is enhanced generally appear in the parts where turbulence is intensified, cavitation phenomenon is significant and eddy current is generated, and the speed of these parts will be significantly different from other parts. Now, the influence of valve Angle and flow channel section length on the heat transfer performance of Tesla valve is analyzed respectively.

Test1, test2, test3, the cross section length of the flow channel of the three experimental groups is 3mm, and their valve angles are 30°, 45°, and 60° respectively. According to the simulation results, Nu at 30° is the highest among the three groups, indicating the best heat transfer effect.

The fluid of the curve and the fluid of the straight passage have impact interaction at the junction, resulting in three low flow rate areas, the pressure drops sharply, the speed increases, resulting in cavitation phenomenon, and then enters the low flow rate area, the pressure increases, and the cavitation bubble disappears. As the valve Angle increases, the Angle of fluid interaction between the bend and the straight passage decreases, and the cavitation effect weakens. As can be seen from the figure, the cavitation region of test2 and test3 is smaller than that of test1, and the cavitation phenomenon can enhance the effect of heat transfer, so the Nu of test1 is the largest among the three.

The heat transfer performance of the Tesla valve is closely related to the flow state of the internal fluid. Under counter current conditions, the flow of fluid inside the valve is impeded, and this obstruction causes the fluid to separate in some parts of the valve, forming a flow separation zone. These separation zones can lead to local stagnation of the fluid, which affects heat transfer efficiency. However, this flow separation also increases the contact time between the fluid and the valve wall, helping to improve heat exchange efficiency. Especially when the flow separation zone is accompanied by the formation of eddy currents, this situation will cause the fluid to further enhance the heat exchange effect with the wall, because the eddy currents can promote the heat mixing and transfer inside the fluid. With the increase of cross section length, Nu value increases and heat transfer performance is enhanced. At the same time, turbulent flow occurs in a larger flow channel, and the probability of eddy current increases. These unstable flows are also responsible for enhanced heat transfer.

The larger the cross section length of the flow channel, the fluid will gradually become obstructed under the condition of forward flow. More and more fluid will enter the curved channel due to inertia, showing the effect of obstructing fluid flow similar to that under the counter current condition, indicating that the increase in the cross section length will increase the probability of fluid entering the curved channel at the intersection of the straight channel and the curved channel. This is not good for optimizing the single pilot connectivity of the Tesla valve.

Changes in the cross section length of the flow channel also affect the heat transfer performance and cavitation phenomenon of the Tesla valve. Increasing the cross section length can increase the heat transfer area and thus improve the heat transfer efficiency. However, excessive cross section lengths may lead to increased impediments to fluid flow, reducing the occurrence of turbulence and eddy currents, and thus reducing heat transfer efficiency. Therefore, the design of Tesla valves requires a balance between heat transfer efficiency and fluid flow resistance.

Equivalent points are set at the entrance, exit, middle interchange and bend of the Tesla valve of test1 and test5, respectively, to monitor the speed and pressure changes in the channel under the condition of forward flow and reverse flow. The specific location is shown in Table 1.

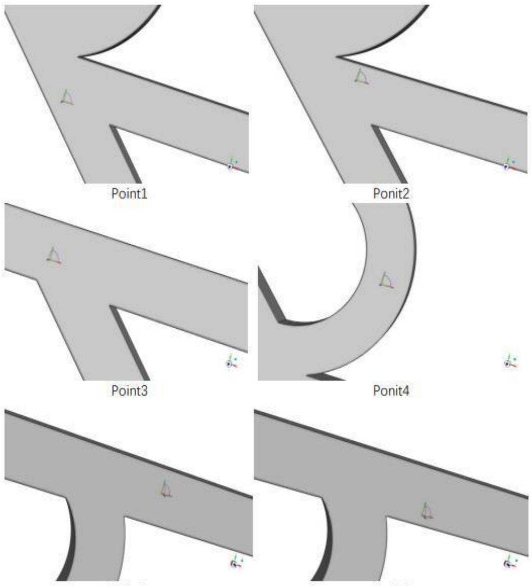

Fig. 2 Set equivalent points

The equivalent points Point1 and Point2 at the middle interchange are used to monitor the velocity difference when the fluid cavitation occurs here in the case of counter current. Subjectively, it is believed that these two points will produce a large velocity difference in the case of counter current, while in the case of forward flow, it will not produce a large velocity difference. The equivalent point Point3 at the entrance is used to monitor the speed at the outlet when the Tesla valve is upstream and the speed and pressure change when the valve is upstream. The equivalent point Point4 is set in the first bend under the counter-current condition to monitor the velocity and pressure change trend of the fluid in the bend under the counter-current condition. The equivalent points Point5 and Point6 are set at the position near the exit of the second bend in the case of counter current, where a temporary cavitation phenomenon may occur. Point6 is set at the core of this low-speed area, and Point5 is located at the high-speed area of the exit of the bend.

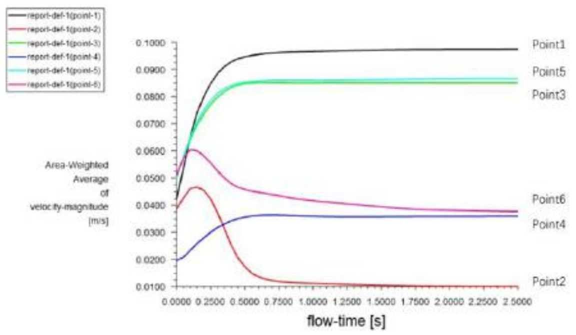

Fig. 3 test1 Reverse flow velocity variation diagram

As shown in Table 2, under the counter current condition of test1, the speed difference between Point1 and Piont2 is the largest, which is consistent with the initial hypothesis. It can be seen from the figure that the speed of Piont2 is close to stable after 1.5s, maintaining at 0.01m/s, while the speed of Point2 is finally maintained at 0.1m/s. The difference between the two is nearly 10 times, and the huge speed difference creates the possibility of cavitation.

Similarly, there is a large speed difference between Point5 and Point6, and the speed of Point4 does not change much. It only takes about 0.5s from the beginning to the final stabilization, which is similar to the stabilization time of Point1, Point5 and Point3. Both Point6 and Point2 are detection points located in the low-speed region. It can be seen that there is a fluctuation in the velocity within 0.025s, which is due to the sudden increase of the fluid velocity in the flow channel, resulting in the fluid velocity in these two low-speed regions being affected until the flow becomes stable. The speed slows down.

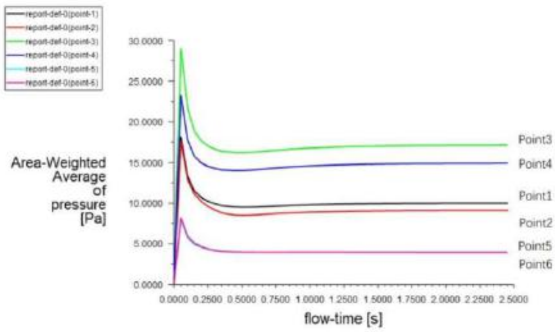

Fig. 4 test1 Reverse flow pressure variation diagram

As can be seen from Fig. 4, the pressure of the Tesla valve system is basically stable after 0.5s, Point3 is the monitoring point at the entrance, and the pressure is the largest. After the fluid enters the bend, the pressure of Point1 and Point2 is close, and the pressure of Point2 is slightly smaller, and the pressure in the cavitation core area is smaller than the surrounding pressure. The pressure of Point5 and Point6 is basically the same, and they are both the monitoring points at the counter current outlet. The pressure of these two points is the smallest or perhaps the difference is very small, which is not easy to see in the figure, and also indicates that the cavitation phenomenon here is not obvious. The counter current velocity pressure is basically stable after 0.75s, the flow of the fluid is basically unchanged, the vortex and cavitation phenomena exist at the same time, due to Angle reasons, the acceleration of the speed at the fluid junction is obvious, and the speed of the bend is basically the same as the inlet speed.

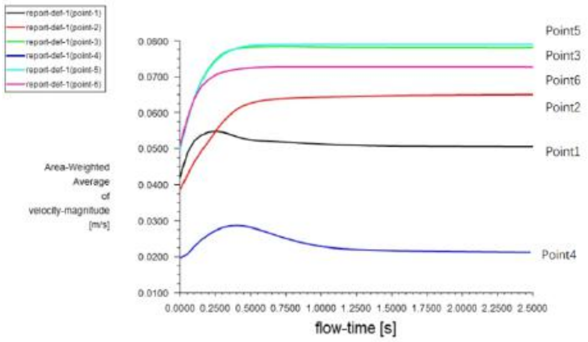

Fig. 5 test1 downstream velocity variation diagram

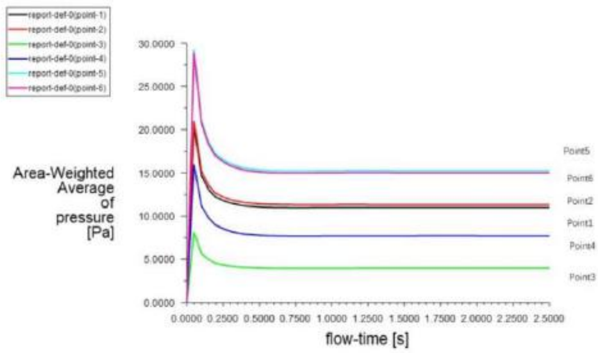

Fig. 6 test1 Up-flow pressure variation diagram

In the case of downflow, as shown in Figure 9, the speed of all monitoring points (except Point4) increases relative to the counterflow. As the monitoring point of the curve, the speed of Point4 is even lower relative to the counterflow, maintaining at about 0.02m/s after stabilization. It can be seen that in the downflow, the fluid does not flow into the curve as much as the counterflow. Point5 and Point6 as inlet monitoring points along the flow, the speed increases obviously. Point1 and Point2 are the monitoring points in the middle of the Tesla valve, and the speed increase is not large in the forward flow, at this time, most of the fluid flows in the straight channel, and the fluid in the bend is less, and the acceleration effect at the intersection is relatively small.

As can be seen from Figure 9, the pressure of similar monitoring points is very close, and the system begins to stabilize at 0.5s, which is much faster than the counter current situation. Only within 0.1s at the beginning, the pressure changes greatly, and the pressure is proportional to the distance from the upstream inlet. The highest pressure is close to 30Pa, and the maximum pressure after stability is about 15Pa. The minimum value is around 4Pa.

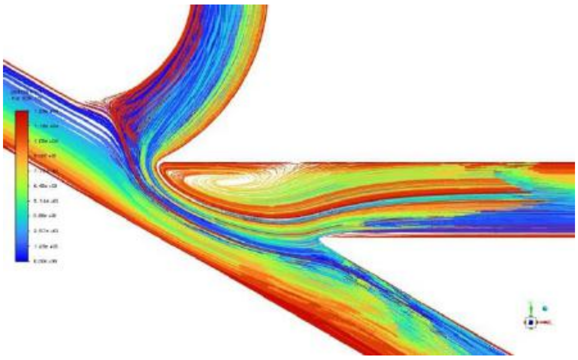

Fig. 7 test1 Particle trajectories at interchanges of counter current

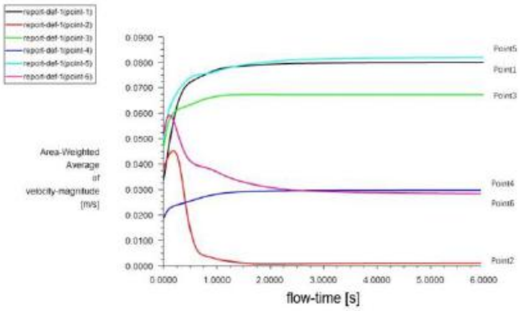

Fig. 8 test5 Reverse flow velocity variation diagram

As can be seen from Figure 8, the complexity of its speed change is much higher than that of test1, but there are still some similarities. For example, the speed difference between Point1 and Point2 is still very large, and the speed difference between Point5 and Point6 is slightly larger than that of test1. The speed of Point5 began to exceed the speed of Point1 after 1.5s, which was very close to the two. However, Point6, which was also in the low-speed area, did not slow down to 0 like Point1 and remained stable at about 0.028m/s. Combined with the speed cloud map, In theory, there should also be a zero-speed region in the low-speed region of Point6 like the middle interchange, which should be because the location of the point is not accurate. If it is really in the core of the low-speed region, the speed should be close to 0 after stability. The increase of the valve Angle and the increase of the flow channel section is beneficial to the stability of the flow of the Tesla valve.

As can be seen from Figure 9, the maximum pressure reaches 25Pa and is about 13Pa after stability. Compared with test1, which has a maximum value of close to 30Pa and a maximum value of 15Pa after stability, test5 has a lower system pressure, which indicates that test5 has a better system stability than test1.

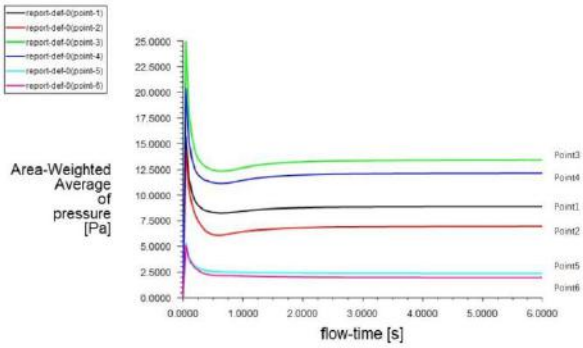

Fig. 9 test5 Reverse flow pressure variation diagram

Point3 is the inlet monitoring point in the case of counter current, the pressure is the highest, the pressure drops after the fluid enters the bend, and finally maintains around 12.5Pa. The pressure difference between Point1 and Point2 is about 2.5Pa, the pressure of Point5 and Point6 is very close to that of the surrounding area, and the pressure in the cavitation core area is smaller than that in the surrounding area. In the case of counter flow, the pressure at the end of the Tesla valve, Point5 and Point6, has decayed to a very low value. Therefore, there is no significant pressure difference between Point5 and Point6, so the probability of cavitation is very low, or the cavitation phenomenon is small and not obvious.

The stabilizing time of the overall pressure is about 1s, which is a little slower than the 0.75s of test1. The increasing of the valve Angle and the size of the channel section may have adverse effects on the stabilizing time.

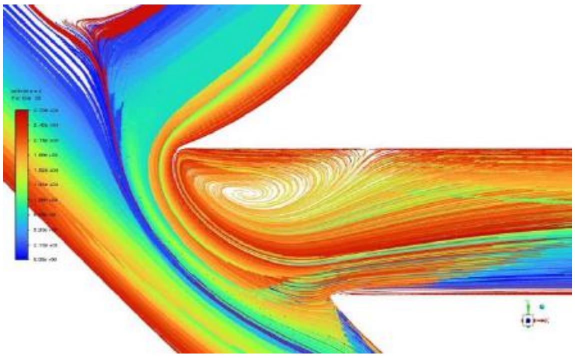

Fig. 13 test5 Particle trajectories at interchanges of counter current

Figure 10 shows that in the case of down flow, the speed of Point4 is the lowest, which is less than 0.02m/s after stability, indicating that in the case of down flow, only a small part of the fluid entering from the entrance flows into the bend, and most of it flows in the straight. Compared with the counter current situation, the speed of Point2 and Point6 both increased in the forward flow, and the speed of Point2 and Point3 was basically the same after stabilization. Before 0.5s, Point1 and Point6 had a fluctuating stage, which first increased and then decreased. In the case of forward flow, the position of Point1 was close to the wall of the straight channel. When the fluid passed through the forward flow, it would impact the wall, and the speed increased for a short time, and then the speed decreased. Point6 is located at the upstream entrance, close to the side wall of the first bend. When the fluid flows through here, a small part of the fluid will enter the bend, resulting in speed attenuation. The speed attenuation of Point6 is larger than that of Point1. At the same position, the Point6 of test1 does not decay, but rises steadily and finally becomes stable. The position of Point6 is not affected by the Angle of the valve, indicating that the increase of the channel section will hinder the co-flow of the Tesla valve, resulting in the non-smooth co-flow.

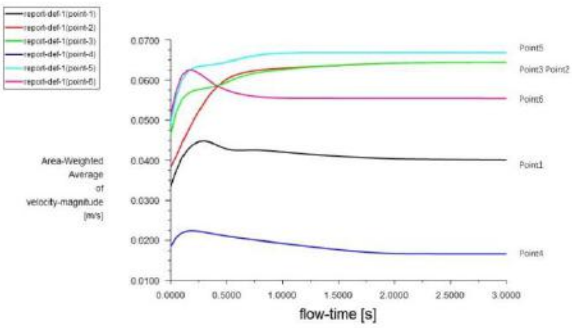

Fig. 10 test5 Up-flow velocity variation diagram

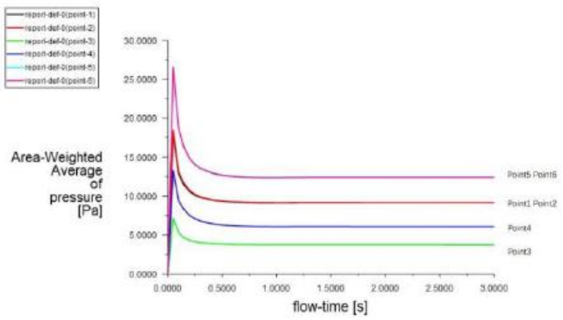

Fig. 11 Downstream pressure variation diagram

Figure 11 shows that the maximum pressure value of test5 is about 27Pa under the condition of downstream flow, and the final stable pressure is about 12Pa, with an intermediate fluctuation of about 15Pa. The minimum value appears at Point3. In the case of down-flow, Point3 is to monitor the pressure at the down-flow outlet, and its value is about 0.4Pa.

The pressure of Point5 and Point6, Point1 and Point2 are completely the same, and the changing trend is the same, indicating that there is no cavitation or vortex phenomenon in the straight channel under the condition of down flow.

The overall pressure of the system becomes stable after 0.5s, which is consistent with the situation of test1 downstream, and the pressure decreases in a step pattern with the distance of the velocity inlet.

4.2 Simulation verification of prediction results

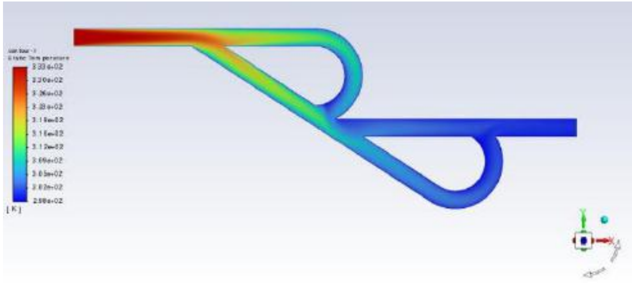

Fig. 12 Prediction group 1 counter current temperature cloud map

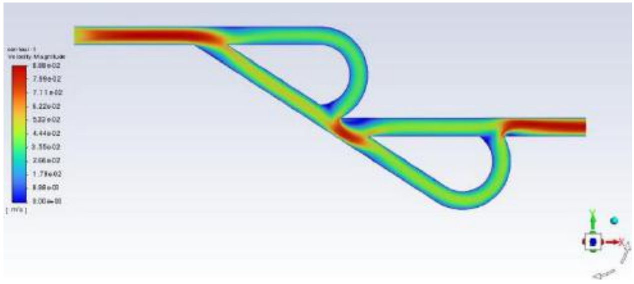

Fig. 13 Prediction group 1 countercurrent velocity cloud map

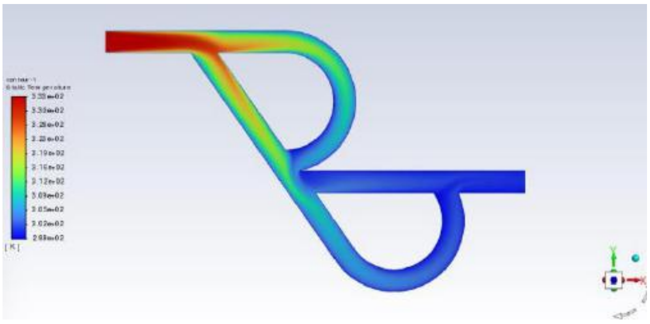

Fig. 14 Prediction group 5 counter current temperature cloud map

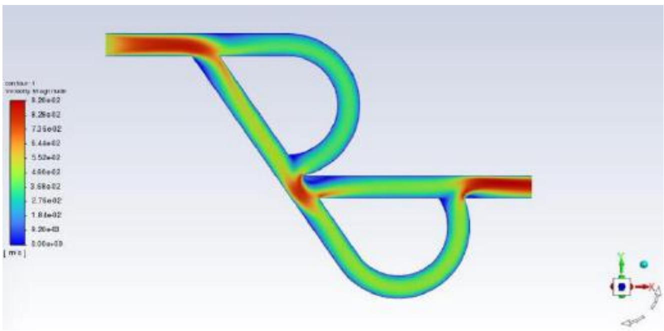

Fig. 15 Forecast group 5 counter current velocity cloud map

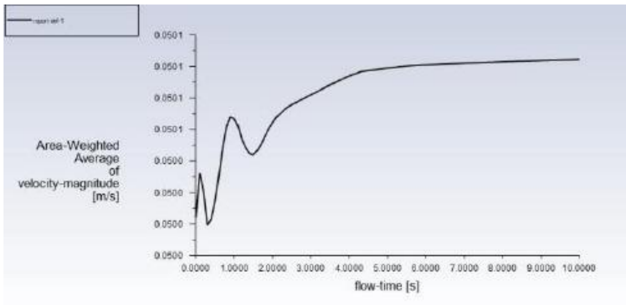

Fig. 16 Forecast group 5 velocity change at counter current outlet

Table 4 Simulation prediction parameter

Forecasting group	Downstream pressure drop ΔPf/Pa	Countercurrent pressure drop ΔPr/Pa	Downstream Nuf	Countercurrent Nur	Di	RPEC
YC1	18.24	19.79	383.87	399.32	1.1	1
YC5	16.57	18.04	272.28	289.17	1.1	1

The results obtained from the training of the neural network were verified. Two sets of data, YC1 and YC5, were selected for simulation verification, and the simulation results of the two sets of predicted data were obtained.

From the velocity and temperature cloud images, their flow conditions and temperature distribution are similar to the previous simulation results.

Combined with the above data, it can be seen that there are still some differences between the simulation data and the training results, and the simulation results are generally greater than the training results, indicating that the training model of the neural network is not as accurate as it is displayed, which may be due to too little training data or inappropriate hidden layers. Or the numerical solution method adopted by Fluent software, such as the finite volume method, is not suitable for discretization and numerical integration, and these steps will introduce certain errors. The selection and setting of numerical methods (such as grid resolution, time step, etc.) directly affect the accuracy of the simulation.

V. CONCLUSION

This research focuses on developing a trained neural network based prediction method to improve the prediction accuracy of the heat transfer mode of the Tesla valve heat sink. The unique design of the Tesla valve heat sink shows its advantages, but the traditional research methods face the problems of complicated calculation, time-consuming and inefficient. By comparing with traditional prediction methods, this study verifies the advantages of the proposed method in terms of calculation efficiency and prediction accuracy, and provides a new possibility for the prediction of heat transfer mode of Tesla valve heat sink.

The results of two Fluent simulations show that the percentage difference of counter current Nu in YC1 is 49.26%, while that in YC5 is 40.93%. This indicates that the difference between the predicted value of YC1 and the simulated value of Fluent is slightly larger than that of YC5. The percentage difference of the Di parameter for YC1 is about 7.29%, while the percentage difference of the Di parameter for YC5 is about 1.43%.

This shows that on the Di parameter, the difference between the predicted value of YC5 and the simulated value of Fluent is smaller than that of YC1. The percentage difference of the RPEC parameters for YC1 is about 7.49%, while the percentage difference of the RPEC parameters for YC5 is about 0.82%. This shows that the difference between the predicted value of YC5 and the simulated value of Fluent is smaller than that of YC1 on the RPEC parameters.

The accuracy of the neural network training model under the known framework is sufficient, and its R value is very close to 1. However, in this study on the heat transfer of Tesla valve, the influence of valve Angle and cross section length on the heat transfer performance of Tesla valve is not a simple linear relationship. There are too few training data, and the differentiation of training data is not fine enough. The activation function or loss function used by the neural network is not suitable, which can lead to inaccurate prediction results. The flow and heat transfer process inside a Tesla valve can involve a variety of complex objects.

ACKNOWLEDGEMENTS

This work described in this paper was supported by the Research Funding of GDUPT, Research on Lagrangian Coherent Structure Analysis of Heat Sink for heat transfer performance with Piezoelectric Fan, Special Project of Taishi Excellent Training Plan in 2024. Special Project of Science and Technology Innovation Strategy of Guangdong Provincial Department of Science and Technology in 2024, (Project No.: 2024A0505050022).

REFERENCES

[1] Hu Zhuohuan, Ding Xiaoyu, Xu Jiayin. Effect of capillary core of Tesla Valve Channel Structure on start-up performance of loop heat pipe (2024). Advances in Chemical Engineering,

[2] Cui Bowen. Research on Flexible Tesla Valve Micromixer with Unidirectional Flow Characteristics (2023), Northeast Dianli University, Jilin, China.

[3] Thompson, S.M., Paudel, B.J., Jamal, T., et al. (2014)

Numerical Investigation of Multistaged Tesla Valves. Journal of Fluids Engineering, 136, 081102-1-081102-9.

[4] De Vries, S.F., Florea, D., Homburg, F.G.A., et al. (2017) Design and Operation of a Tesla-Type Valve for Pulsating Heat Pipes. International Journal of Heat and Mass Transfer, 105: 1-11.

[5] De Vries, S.F., Florea, D., Homburg, F.G.A., et al. (2017) Design and Operation of a Tesla-Type Valve for Pulsating Heat Pipes. International Journal of Heat and Mass Transfer, 105: 1-11.

[6] Qin Suhui. Finite-time and Fixed-time Stability Analysis of a Class of neural Networks (2022), Shanghai University of Finance and Economics, Shanghai, China.

[7] Xun Kangdi, Li Xingcheng, Liu Kelei et al. Mobile phone graphite heat sink defect detection based on machine vision (2022). Journal of Shaanxi University of Technology (Natural Science Edition).

[8] Shen Yuanchu. Research on Multi-stability problems of several kinds of neural Networks (2022), Xuzhou, China University of Mining and Technology.

[9] Wen Ting. Finite-time and Fixed-time synchronization analysis of several types of neural Networks (2022.)., Huangshi, Hubei Normal University, China.

[10] Ren Pu, Long Wei. Numerical analysis of Flow Field Characteristics and Cavitation formation Mechanism of Tesla Valve (2021). Journal of Southwest University (Natural Science Edition)

[11] Qian Jinyuan, Chen Minrui, Li Xiaojuan et al. Numerical Study of Heat Sink Heat Transfer Enhancement in Tesla Valve Microchannels (2020) Fluid Machinery,

[12] Qian Jinyuan, Chen Minrui, Li Xiaojuan et al. Numerical Study of Heat Sink Heat Transfer Enhancement in Tesla Valve Microchannels (2020) Fluid Machinery,

[13] Zhou Runzhong, Qiao Yujie, Zhang Yuxiang et al. Simulation of Tesla Valve Performance (2020). Physical experiments

[14] Wang Tao, Wang Haowen, Lin Yuchen, et al. Numerical Study on Hydraulic Cavitation of Tesla Valve (2020) Journal of Chemical Engineering of Universities 34

[15] Feng Haojie. Dynamic Behavior Analysis and Application of Neural Networks (2020), Zhongyuan University of Technology, Zhengzhou, China

[16] Zhang Xiaoling. Dynamic Analysis of Two Kinds of Neural Network Models (2020), Changsha University of Science and Technology, China

[17] LIU Haiyang, Ma Jia, Wang Sen et al. Research on Single pilot Connectivity of Tesla Valves (2020). Physics and Engineering 120-124.